Journal of Engineering and Sustainable Development

Vol.20, No.03, May 2016
ISSN 2520-0917
www.jeasd.org

COMPARATIVE STUDY OFTHE LEAD (II) REMOVAL FROM SIMULATED WASTEWATER USING GRANULAR ACTIVATED CARBON, RISE HUSK, AND SAW DUST

*Younis Swadi Talaa

Asst. Lect., Environmental Eng. Dept., Al-Mustansiriayah University, Baghdad, Iraq**.**

(Received: 08/09/2015; Accepted: 27/12/2015)

Abstract: The adsorption of Pb (II) ions onto Granular Activated Carbon (GAC), Rise Husk (RH) and Saw Dust (SD) was investigated. The effect of pH, initial lead (II) concentration, dose of adsorbents, contact time and temperature were studied in batch experiments. The equilibrium data were analyzed using Langmuir, Freundlich and sips isotherm models at different doses of GAC, RH, and SD. The Langmuir model was found to fit the equilibrium data very well with high-correlation coefficient (R^2). The maximum uptake capacities were found to be 6.823, 63.044, and 10.046 mg/g onto GAC, RH, and SD, respectively. Adsorption kinetic data were tested using pseudo-first-order, pseudo-second-order, and intra-particle diffusion models. The adsorption process was found to follow a pseudo-first order reaction. Thermodynamic parameters such as Gibbs free energy change, Enthalpy change and Entropy change have been calculated. These thermodynamic parameters indicated that the adsorption process was spontaneously under natural conditions and the adsorption was endothermic in nature. The study showed that locally available adsorbents, such as RH and SD, can be used as efficient adsorbents for the removal of lead (II) as compared with commercial GAC.

Keywords: *Adsorption; lead (II); Granular Activated Carbon (GAC); Rise Husk (RH);Saw Dust (SD); Langmuir; Pseudo-first-order*

دراسة مقارنة لأزالة الرصاص (II) من المياه الملوثة المصنعة بإستخدام الكاربون المنشط الحبيبي، قشور الرز و نشارة الخشب

الخلاصة: تم في هذا البحث دراسة عملية أمتزازألرصاص (II) بأستخدام كلاً من الكاربون المنشط الحبيبي (GAC)، قشور الرز(RH) ونشارة الخشب (SD). تأثير كلاً من الدالة الحامضية (pH)، التركيز الابتدائي للرصاص (II)، جرعة المادة المازة، وقت التفاعل ودرجة الحرارة تم دراستهابأستخدام تجارب الدفعة الواحدة. نتائج التوازن تم تحليلها بأستخدام موديلات لانكَمير، فريندلج وسب عند جرع مختلفة من كل من الكاربون المنشط الحبيبي، قشور الرز ونشارة الخشب. من بين هذه المديلات وجد ان موديل لانكَمير ينطبق على النتائج العملية وبمعامل ارتباط عالي. أن اكبر سعة أمتزاز كانت 6.823، 63.044 و 10.046 ملغم/غم لكل من الكاربون المنشط الحبيبي، قشور الرز ونشارة الخشب بالتتابع. موديلات الحركة تم أختبارها من خلال تطبيق موديلات الدرجة الاولى والدرجة الثانية الافتراضية وموديل الانتشار داخل الدقائق ومن بين تلك الموديلات وجد ان عملية الامتزاز تتبع موديل الدرجة الاولى الافتراضي. محددات الحرارة مثل الطاقة الحرة لكَبس، الطاقة الكامنة، الطاقة المتحررة تم حسابها ومن خلالها تم أستنتاج ان عملية الامتزاز هي عملية تلقائية تحت الظروف الاعتيادية وان التفاعل هو من النوع الماص للحرارة. الدراسة بينت أمكانية أستخدام كلاً من قشور الرز ونشارة الخشب كمواد مازة محلية وكفؤءة نسبياَ مقارنة بالكاربون المنشط التجاري لازالة الرصاص (II).

---

* eng.younis82@yahoo.com

1. Introduction

According to the World Health Organization (WHO), the metals of most immediate concern are aluminum, chromium, manganese, iron, cobalt, nickel, copper, zinc, cadmium, mercury and lead. In special, lead is one of the important toxic elements found in the industrial effluents causing water contamination; possibly enters to the ecosystem through soil, air and water. Inorganic lead causes disturbance in the cardinal neural system by modifying the features of the early organism [1, 2]. According to WHO, the maximum allowable limit of lead in drinking water is 0.1 mg/L [3].Hence, the appropriate handling of industrial wastewater which releases lead into the aquatic and terrestrial systems is real significant.

At present, a number of technologies can be practiced to get rid of heavy metals from the contaminated wastewater such as filtration, adsorption, chemical precipitation, ion exchange, membrane separation, and electro remediation methods [4,5].Nevertheless, most of these methods might not be effective in getting rid of heavy metal at very low concentrations, and could be relatively expensive. These methods are also not efficient due to their secondary effluent impact on the recipient environment. Hence, the simple, effective, low price and eco-friendly techniques are demanded for the fine tuning of effluent wastewater treatment.

The search for low cost, and easily available adsorbents has led to the investigation of materials of agricultural and biological origin, alongside those of industrial by-products as adsorbents for removal of heavy metals [6,7].The objective of the present work was to investigate adsorption characteristics for the removal of Pb^{2+} from simulated wastewater by the use of low-cost abundantly available nonconventional adsorbents such as rice husk (RH) and sawdust (SD) and compared with granular-activated carbon (GAC) adsorption capacity.

2. Methods and materials

2.1. Adsorbents preparation

Commercial granulated activated carbon (GAC) (trade mark Unicarbo, Italians) was bought from the local market. GAC was washed before being used with distilled water to remove fine powder and then dried in an oven at 110°C for 24 hours, after which the GAC is kept in a desiccator for use. The rice husk (RH) was collected from Al-Shamiyyah rice mill located in Al-Diwaniya where large quantities of residual rice husk were produced in the production of rice. The Sawdust (SD) was collected from several furniture fabrics in Baghdad, where large amount is produced as residuals from production of different furniture. This was washed with double distilled water to remove water-soluble impurities and surface-adhered particles. Then the adsorbent was oven-dried at 60°C to remove the moisture and other volatile impurities.

The physical and chemical properties of adsorbents are measured at the laboratories of the Ministry of Industry and Minerals (Ibn Sina State Company), Ministry of Oil (Petroleum Development and Research Center), Al-Mustansiriayah University (College of Engineering, Environmental Department) and according to the data from the supplier and listed in Table1. The specific surface area and total pore volume were evaluated utilizing the multi-point-N2-Brunauer, Emmett and Teller (BET) method (Surface area analyzer, BET method, Quantachrome.com, USA). The functional groups of GAC, DB, and PR were detected by FT-IR analysis. The proportion of adsorbent/KBr is 1/100. The background is obtained from the scan of pure KBr. FT-IR spectrophotometer, IRPRESTIGE-21, SHIMADZU, Japan was used for analysis. Phases present in the samples (chemical analysis) were examined using an X-ray diffractometer (PAN analytical X-ray, Philips Analytical, Germany) and present in Table 2.

Table 1.Physical and chemical prosperities of GAC, RH, and SD

Specifications	Adsorbents		
	GAC	RH	SD
Source	Uncarbo company Italy form local markets	Local Iraqi mills	Collected from a local furniture factory
Origin	Coco nut shell	Rise milling waste	Sawmill waste
Surface area(m^2/g)	352	50.15	10.17
Particle porosity	0.48	0.43	-
Mean particle	0.78	0.78	0.78
Pore volume, cm^3g^{-1}	0.422	0.184	-
CEC meq/100 g	-	80.43	43.118
pH	8.74	-	-

Table 2.Chemical analysis of GAC, RH, and SD samples

GAC		R.H		S.D	
Constituent	Wt.%	Constituent	Wt.%	Constituent	Wt.%
C	88.77	SiO2	96.36	SiO_2	86.1
O	10.51	MgO	0.4	$CaSiO_3$	2.9
Si	0.28	Al_2O_3	0.42	MgO	2.6
S	0.05	K_2O	2.30	Al_2O_3	4.4
K	0.18	CaO	0.42	SO3	2.1
Ca	0.21	Fe_2O_3	0.1	L.O.I	1.9

2.2. Preparation of Lead (II) solution

A standard solution of lead with concentration of (1000 mg/l) was prepared using $Pb(NO_3)_2$ salt. A (1.5985 g) of this salt was dissolved in about 200 ml of distilled water.A 10 ml concentrated HNO3 was added then it was reduced to 1000 ml with distilled water and storing it in glass container at room temperature [8]. Working solutions of 10, 25, 50, 75 and 100 mg/L were prepared by dilution. And the specific concentration was measured using atomic absorption spectrophotometer (AAS).

2.3. Batch adsorption experiments

The specified adsorbent was placed in 250mL bottles containing 100mL of lead (II) solution. The bottles were then put on a shaker and agitated continuously at 200 RPM for the desired pH value, contact time, and adsorbent dosage level.Different initial concentration of Pb^{+2} solutions was fixed by proper dilution from stock 1,000 mg/L. pH of the solution monitored by adding 0.1N HNO_3 and 0.1N NaOH solutions as per required pH value. Necessary amount of adsorbent material was the added, and contents in the flask were shaken for the desired contact time at ambient temperature (i.e. 20 ± 2°C). The contents of the flask were filtered through filter paper and filtrate was analyzed for Pb^{+2} .The percentage removal of Pb^{+2}were calculated as follows:

$$RE\,(\%) = \frac{C_o - C\text{eq}}{C_o}\,\% \qquad (1)$$

Where: C_o and C_{eq} are the initial and final concentration of the metal ion (mg/L).

2.4. Adsorption Isotherms

The equilibrium established between adsorbed component on the adsorption and unadsorbed component in solution can be represented by adsorption isotherms. The most widely used isotherm equations for modeling equilibrium is the Langmuir equation which is valid for monolayer sorption onto a surface a finite number of identified sites and is given by Eq. (2):

$$q_e = \frac{q_m b C_e}{(1 + bC_e)} \qquad (2)$$

Where: q_e is the amount of pollutant bound to per g of adsorbent at equilibrium and C_e is the residual (equilibrium) pollutant concentration left in solution after binding, respectively. q_m is the maximum amount (maximum loading capacity) of pollutant per unit weight of the adsorbent to form a complete monolayer on the surface bound at high C_e, and b is a constant related to the affinity of the binding sites [9].

The Freundlich expression is an empirical equation based on sorption on a heterogeneous surface, suggesting (as expected) that binding sites are not equivalent and/or independent. The mono-component Freundlich equation is presented below by Eq. (3):

$$q_e = KC_e^{\,1/n} \qquad (3)$$

Where: K_F and n are the mono-component Freundlich constants characteristic of the system [10].Sips model (Combination of Langmuir-Freundlich Model:

$$q_e = \frac{bq_m C_e^{1/n}}{1 + bC_e^{1/n}} \qquad (4)$$

Where *b* (L/mg) is a constant related to the affinity of the binding sites and *n* are the mono-component Freundlich constant characteristic of the system [11].

2.5. Adsorption and kinetics

The kinetic parameters for the adsorption process were examined on the batch adsorption of 50 mg/L of Pb^{+2} at pH 5.The contact time was changed from 30 to 300 minute, and the percentage removal of Pb^{+2} was monitored during the survey. The data were fitted to different kinetics adsorption models:

2.5.1. Pseudo-first-order kinetic model

The Lagergren rate equation was the first-rate equation for the sorption of liquid/solid system based on strong capacity and this model represent physical adsorption for pollutants onto adsorbent surface [12]:

$$\log(q_e - q_t) = \log(q_e) - \frac{K_L}{2.303}t \qquad (5)$$

where q_e is the amount of Pb^{+2} adsorbed at equilibrium(mg/g); q_t is the amount of Pb^{+2} adsorbed at time t (mg/g); and k_L is the equilibrium rate constant of pseudo-first sorption (min^{-1}).

2.5.2. Pseudo-second-order kinetic model

If the sorption rate of system is a pseudo-second order mechanism, the rate-limiting step may be chemical sorption or chemisorptions involving valency forces through sharing or the exchange of electrons between adsorbent and adsorbate as covalent forces [12]:

$$\frac{t}{q_t} = \frac{1}{K_2 {q_e}^2} + \frac{1}{q_e}t \qquad (6)$$

Where k_2 (g/mg.min) is the rate constant of adsorption.

2.5.3. Intra-particle diffusion model

The intra-particle diffusion model is expressed as [12]:

$$q_t = K_{id}t^{1/2} + C \qquad (7)$$

Where k_{id} (mg/g $min^{1/2}$) is the rate constant of intraparticle diffusion, C is the value of the intercept which gives an idea about the boundary layer thickness, that is, the larger intercept; the greater is the boundary layer effect. The linear plots of q_t vs. $t^{1/2}$ with zero intercept indicate that intra-particle alone determines the overall rate of adsorption. In this case, intra-particle diffusion is not the only determining mechanisms; in addition, other mechanisms such as electrostatic interaction, ion exchange may be operating to different extents.

2.6. Adsorption thermodynamics

Based on fundamental thermodynamic concepts, it is assumed that in an isolated system. Energy cannot be realized or missed and the entropy change is the sole driving force. The apparent the equilibrium constant for the process has been shown to be [13]:

$$\Delta G^{o} = -RT\ \mathrm{Ln}\ (KC) \qquad (8)$$

$$Kc = \frac{Co-Ceq}{Ceq} \qquad (9)$$

Also, enthalpy changes (ΔH^{o}) and entropy changes (ΔS^{o}) can be estimated by the following equation:

$$\Delta G^{o} = \Delta H^{o} - \Delta S^{o}T \qquad (10)$$

Where ΔG° is standard Gibbs free energy change in kJ/mol; ΔH° is change in enthalpy (heat ofAdsorption, KJ/mole), ΔS° is the change in entropy in KJ/Mol, R is the universal gas constant (=0. 8314KJ/Mol. K) and T is the temperature in K.

3. Results, discussion and conclusion

3.1. Effect of pH

The pH of the metal solution usually plays an important role in the absorption of metals. Beyond the value of pH 6.0 precipitation will occur to heavy metals, this due to the insoluble metal hydroxides start precipitating from the results at higher pH values and establish the true sorption studies impossible. This should be avoided during sorption experiments which distinguish between sorption and precipitation metal removal becomes hard [14]. Thus, the uptake of Pb^{+2} as a function of pH was examined over a range of (2–6) as shown in Fig.1.

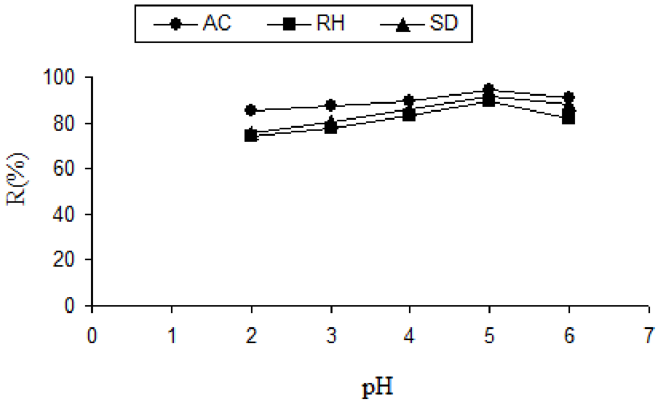

Figure. 1. Effect of pH on the adsorption of Pb^{2+} by GAC, RH and SD, initial concentration 50 mg/L, adsorbent dose 1 g, contact time 3.5 h and temperature 20°C.

The effect of pH can be explained considering the surface charge on the adsorbent material. At low pH, proton would compete for active binding sites with metal ions. The protonation of active sites thus tends to decrease the metal sorption. At low pH around 2 all the binding sites may be Protonated, thereby desorbing all originally bound metals from the biomass [15].Further, increasing the pH causes decreasing of negatively sites and thus reduce removal efficiency [16]. The maximum equilibrium uptake values obtained at pH 5.0 for GAC, RH and SD were 94.17, 91.56 and 89.47% respectively. Hence, pH 5 was thought to be the optimum pH for further experiments.

3.2. Effect of adsorbent mass

The effect of varying the adsorbents mass on the adsorption of lead ions is shown in Fig. 2. Removal efficiency increases in lead (II) from (77.08 to 99.9%) onto GAC, (74.72 to 97.98%)onto SD and (72.23 to 95.79%)onto RH as the mass increases from 0.5 to 3g. The rate of increase gradually decreases with increasing adsorbent mass above 2g. It is distinctly understood that the removal efficiency increases as the adsorbent mass increases. With increasing adsorbent dosages, more surface area is available for absorption. As the adsorbent mass increases, the number of binding sites for the ions also increases. Later on some point, sorption capacity was steady or due to a screen effect between adsorbent, this brought out a blockage of the adsorbent active sites by an increase in lead ions in the system [32].

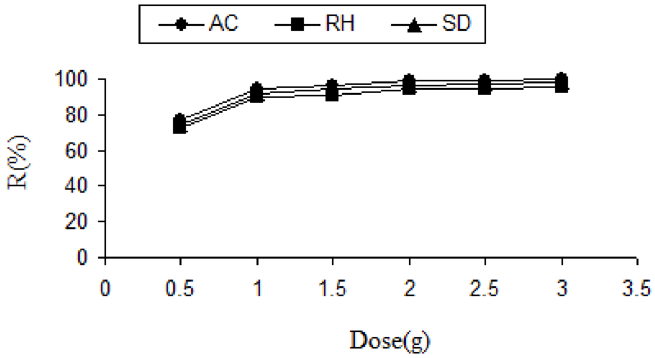

Figure 2. Effect of adsorbent dose on the adsorption of $Pb^{+2}$by GAC, RH and SD, pH 5, initial Pb^{+2}concentration 50 mg/L, contact time 3.5 h and temperature 20°C.

3.3. Effect of initial metal ion concentration

The feasibility and efficiency of an adsorption process depends not only on the properties of the adsorbents, but also on the concentration of the adsorbate.The initial metal concentration provides an important driving force to sweep over all mass transfer resistances of the metal between aqueous and solid form. The effect of initial concentrations of Pb^{+2} was studied and illustrated in Fig.3. The efficiency values decrease from 99.93 to 70.63% for Pb^{+2} onto GAC, from 98.82 to 61.14% for Pb^{+2} onto SD and from 97.65 to 58.25% for Pb^{+2} onto RH as the initial concentration increased from 10 to 100 mg/L. At lower metal ions concentration, the percentage uptake was higher due to larger surface area of Sorbent being available for sorption. When the concentration of metal ions became higher, the percentage removal has decreased since the available sites for sorption became less due to saturation of sorption sites. At a higher concentration of metal ions, the ratio of initial number of moles of metal ions to the sorption sites available was high, resulting in a lower sorption percentage [18].

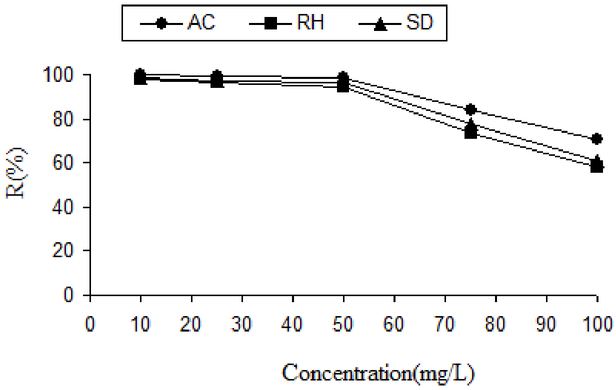

Figure 3.The effect of initial concentration on the adsorption of Pb^{+2} by GAC, RH and SD, pH 5, adsorbent dose 2 g, Contact time 3.5 h and temperature 20°C

3.4. Effect of contact time

Contact time plays an important role in the efficient removal of Lead ions using different adsorbents. The influence of contact time on the adsorption capacity for different metal ions is shown in Fig. 4. Removal efficiency increases for Lead from 40.32 to 98.14% onto GAC, 30.87 to 95.21% onto SD, and 25.65 to 90.32% onto RH as the contact time increases from 15 to 240 minute. The results clearly revealed that rate of absorption is higher at the outset and this is due to availability of a large bit of active sites on the adsorbents. As these sites are exhausted, the uptake rate is controlled by the rate at which the adsorbent is transported from the exterior to the interior sites of the adsorbent particles [19]. Maximum removals were attained within the first 180 min of stirring times. There must not be seemed to be much benefit after 270 min. Thus, the equilibrium time was set to be 3.5 h.

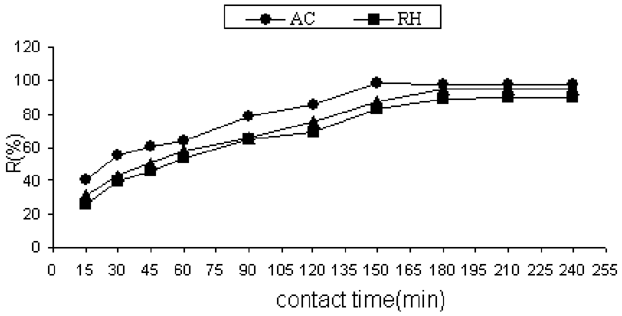

Figure 4. Effect of contact time on the adsorption of Pb^{+2} by GAC, RH and SD, pH 5, initial Pb^{2+} concentration 50mg/L, adsorbent dose 2 g and temperature 20°C.

3.5. Adsorption isotherm models

The parameters for each model were estimated by nonlinear regression using STATISTICA version-6 software. All parameters with correlation coefficient are summarized in Table 3. The adsorption isotherms for Pb^{+2} onto GAC, RH, and SD are shown in Figs. 5,6 and 7. From these Figures and Table 3, the following conclusions can be drawn: Langmuir model gave the best fit for the experimental data for lead(II) adsorption with correlation coefficients of 0.989, 0.993, and 0.988 onto GAC, SD, and RH, respectively. The maximum adsorbed amount (q_m) for Pb^{+2} onto the selected adsorbents follow the sequence as: q_m RH> q_mSD> q_m GAC as determined in Table 3.Cationexchange capacity (CEC) for RH represents the total quantity of lead cation that can be replaced by positive ions (K^+, Na^+, Ca^{2+}, and Mg^{2+}) on RH.CEC for RH used in this survey was 80.43 meq/100 g [20]. Thus, adsorption capacity for RH exceeds that for GAC and SD.

Table 3. Parameters of adsorption isotherm for lead ions onto GAC, RH, and SD

Model	Parameters	A.C	R.H	S.D
Freundlich	K, (mg/g) (L/mg)$_{(1/n}$	2.789	0.671	1.720
	N	3.427	0.998	1.861
	R^2	0.960	0.995	0.997
Langmuir	q_m(mg/g)	6.823	63.044	10.047
	b(L/mg)	0.655	0.118	0.166
	R^2	0.958	0.993	0.991
	R_L	0.307	0.249	0.373
Combination of Langmuir-Freundlich	q_m (mg/g)	9.291	96.954	9.032
	b $(L/mg)^{1/n}$	0.434	0.007	0.173
	N	1.779	0.954	0.883
	R^2	0.968	0.990	0.982

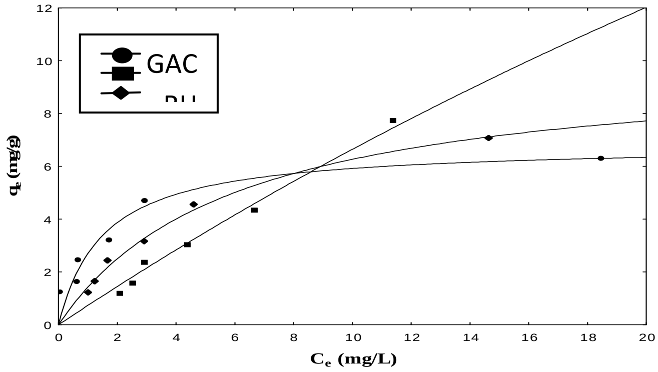

Figure 5.Adsorption isotherm of lead ions onto GAC, RH and SD in single system.

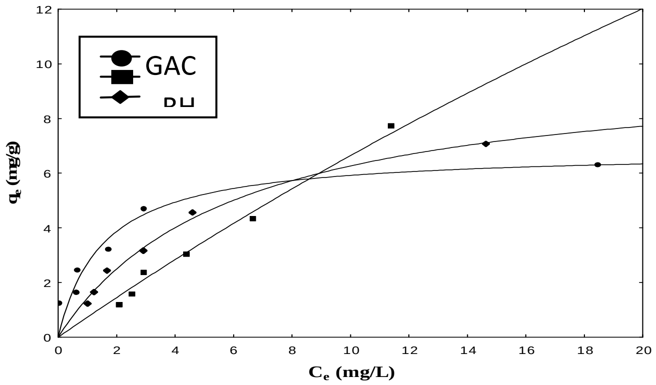

Figure 6.Adsorption isotherm of lead ions onto GAC, RH and SD in single system.

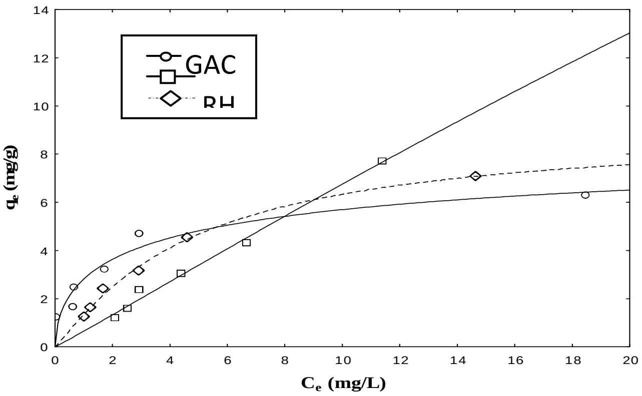

Figure 7.Adsorption isotherm of lead ions onto GAC, RH and SD in single system.

A comparison of the maximum adsorption capacity (q_m) of the GAC, RH and SD sample with that of some other adsorbents reported in the literature are given in Table 4. The adsorption capacity of the RH and SD samples was relatively high when compared with other adsorbents.

Table 4. Adsorption capacities (qm, mg/g) for lead(II) of various adsorbents

Adsorbent	Pb^{2+} qm (mg/g)	References
Kaolinite	1.14	[21]
Cement Kiln Dust	2.445	[22]
Sand	0.169	[23]
Porcelanite	76.104	[24]
Bentonite	36.4	[25]
Dried activated sludge	83.5	[26]

3.6. Adsorption rate kinetics, mechanisms

The subject field of adsorption kinetics describes the solute uptake rate and evidently these rate controls the residence time of adsorbate uptake at the solid–solution interface including the dissemination process. The mechanisms of adsorption depend mass transfer operation. The kinetics of lead ions adsorption onto GAC, SD, and RH were analyzed using pseudo-first-order, pseudo-second order, and intra-particle dispersion models.Table 5 shows the results of these exemplars. The rate of Pb (II) adsorption on the three adsorbents observed to follow the first-order rate law derived by Lagergren Eq. (5). Figs. 6 and 7 show the Lagergren plot of log(qe _qt) vs. time (min) and effluent concentration (Ce) vs. time (min) for all adsorbents. The linearity of these plots suggests that a first-order mechanism is indeed fall out in this process and that the process is physical rather than being chemical which represent by second-order kinetic model. Nevertheless, the value of constant (C) in the intraparticle diffusion model is not equal to zero, suggesting that adsorption proceeds from boundary layers mass transfer across the interfaces to the intra-particle diffusion within the pores of adsorbent. This indicates the mechanism of lead (II) adsorption is complex and both the surface adsorption and intra-particle diffusion contributes to the rate-determining step [27].

Table 5.Kinetic model parameters for Pb^{+2} ions adsorption onto GAC, RH, and SD

Model	Parameters	A.C	R.H	S.D
Pseudo-first-order Equation	q_{eq}(mg/g)	1.315	1.844	1.7297
	K_L(1/min)	0.011	0.012	0.030
	R^2	0.987	0.991	0.994
Pseudo-second-order Equation	q_{eq} (mg/g)	2.979	5.824	5.770
	K_s(g/mg.min	0.0096	0.0027	0.0031
	R^2	0.928	0.969	0.970
Intraparticle diffusion Equation	C	0.573	0.106	0.363
	K_{id}(mg/g.min$^{0.5}$)	0.152	0.326	0.318
	R^2	0.981	0.983	0.977

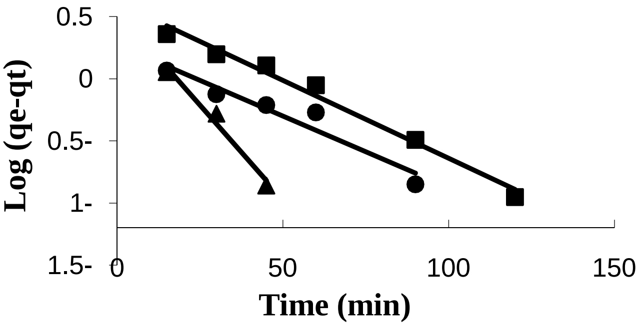

Figure8: Pseudo-first order model for adsorption of lead ions onto GAC, RH and SD in single system

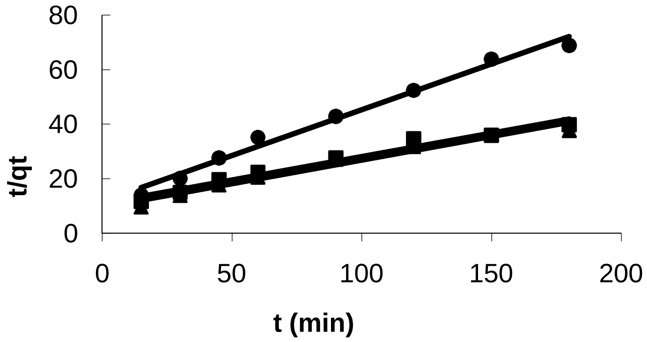

Figure 9: Pseudo-second order model for adsorption of lead ions onto GAC, RH and SD in single system

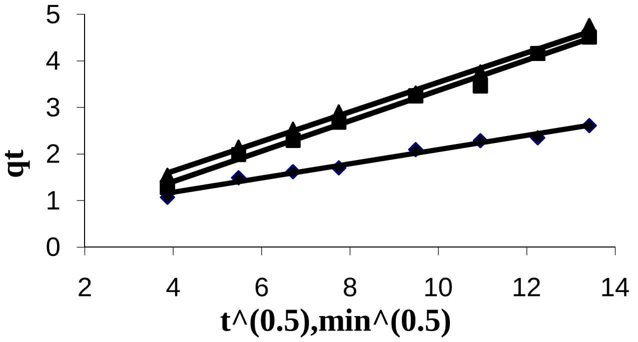

Figure10: Intra-particle diffusion model for adsorption of lead ions onto GAC, RH and SD in single system

3.7. Thermodynamic for adsorption process

The thermodynamic equilibrium constant Kc obtained from calculating the apparent equilibrium constant Kc at different initial concentration of lead (II) and extrapolating to zero. The Gibbs free energy for the adsorption process was obtained at 30° C using Eq. (8), Table 6 The Gibbs free energy indicates the degree of spontaneity of the adsorption process, where more.

Table 6 Thermodynamic constants of adsorption obtained for Pb^{2+} ions adsorption onto GAC, RH, and SD

	Temperature(K)	$-\Delta G^{\circ}(kJ.mol^{-1})$	$-\Delta H^{\circ}(kJ.mo1^{-1})$	$-\Delta S^{\circ}(J.mol^{-1}K^{-1})$	R^2
GAC	393	8.40775	35.835	0.0953	0.936
	303	6.54073			
	313	5.6522			
	323	5.06552			
	333	4.3808			
SD	393	7.91643	35.831	0.0975	0.897
	303	5.73672			
	313	4.91099			
	323	4.22838			
	333	3.79628			
RH	393	6.21454	27.594	0.0733	0.9702
	303	5.4828			
	313	4.48332			
	323	3.69389			
	333	3.44611			

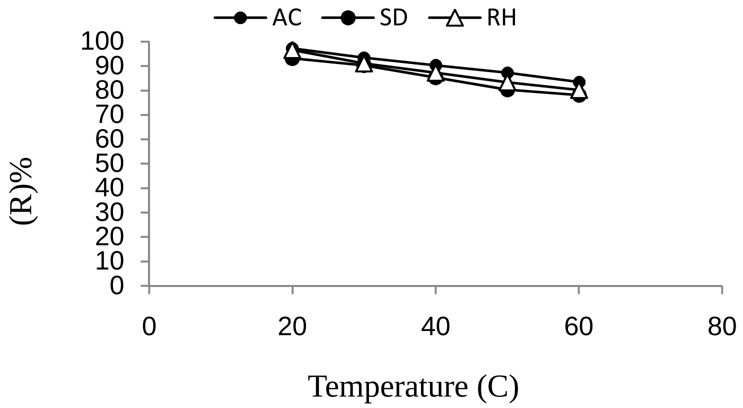

Figure 11. Effect of temperature on the adsorption of Pb^{2+} by GAC, RH and SD, pH 5, initial Pb^{2+} concentration 50 mg/L, adsorbent dose 2 g.

Negative values reflect a more negatively favorable adsorption process. The Gibbs free energy values were obtained as -8.408, -6.214, and -7.916 kJ.mol $^{-1}$ which corresponds, respectively, to GAC, RH, and SD. The negative ΔG° values indicated the feasibility of these adsorbents and spontaneity of the adsorption. And that the adsorption process is exothermic in nature [12].

3.8 Mechanism of metal ions adsorption by GAC, RH, and SD

In order to find out which functions are responsible for lead(II) adsorption, FT-IR analysis of GAC, RH, and SD was carried out. Figs. 12–14 show the spectra of raw and treated adsorbate samples. The FTIR spectra of GAC in the range of 500– 4,000 cm^{-1} shows less intensity in functional groups that responsible for adsorption process compared with RH and SD. From the results depicted in Fig. 12, it can be concluded that the band between 3402.43–2360.87 indicating the presence of OH and NH groups, the C=O stretching of carbonyl in carbonized acid at1643. 35 cm^{-1}, C=C stretching of the aromatic compound and alcohol at 1516.05 cm^{-1}, and C–O is stretching of carboxylic acid at 16 cm^{-1} and other groups [28]. Nevertheless, the GAC is used efficiently for organic pollutant removal. Ali et al., compare the adsorption capacity of the GAC towards lead (metal ion) and phenol (organics). They found that, the maximum loading capacity (q_m) of the phenol was 66.8234 mg/g while it was just about 37.0370 mg/g, for lead. These behaviors due to limited functional groups responsible for metals adsorption onto activated carbon surface by electrostatic attraction [28].

The infrared spectrum of the RH that is shown in Fig. 13 presents typical silica bands. The band with maximum at 1100 cm^{-1} is due to Si–O stretching vibration modes, the band at 800 cm1 is attributed to the ring structure of SiO4 tetrahedra of silica and the band at 475 cm^{-1} is assigned to deformation of Si-O-Si. The band present at 3400 cm-1 is due to the O–H stretching of the silanol SiOH groups on the silicon oxide surface. It can be also observed a small fraction of residual organics from the C–H stretching at 2925 cm1. Consequently, the infrared analysis indicates that the RH adsorbent is a fabric with high content of SiO2 and very low contents of organic components [29].The FTIR spectrum of sawdust given in Fig. 14 showed small absorption bands at 3726.2, 3618.2 and 3525.6 cm^{-1} assuming the presence of H-bridges and crystal water. A medium band at 2908.5 cm^{-1} was also attributed to H- bridges, the weak band at 2125.4 cm^{-1} may be attributed to (C=CH) while the band at 1639.4 cm^{-1} was due to (C=C).The strong band observed at 1033.8 cm^{-1} indicated the stretching of the many C-OH and C-O-C bonds. The decrease and increase in intensities at particularly peaks define the change in the structure with Cd2 and imply the related functional groups to be responsible for the adsorption [30].

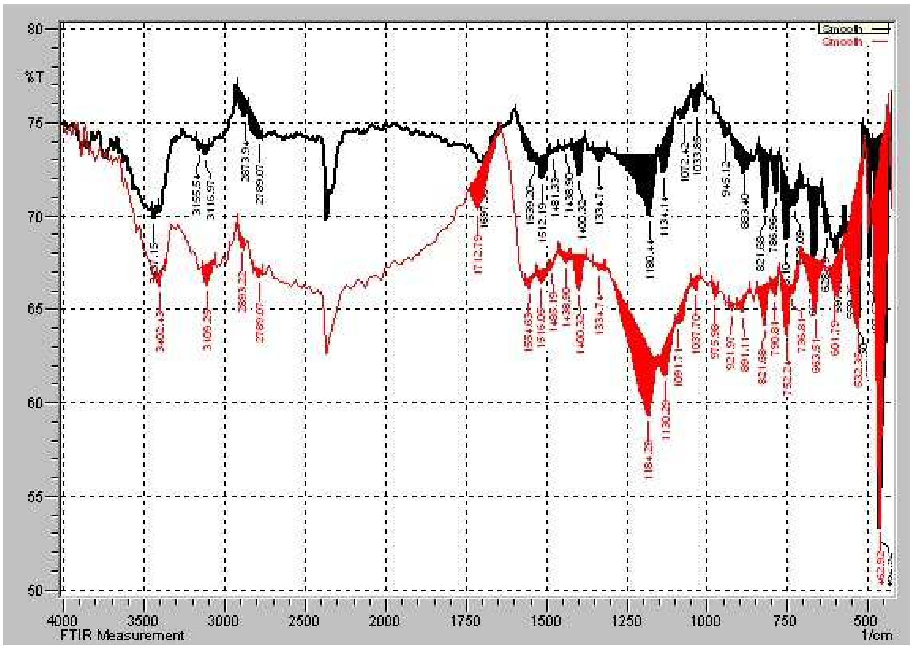

Figure12. FTIR spectra of GAC (1) before, (2) after Pb^{+2} adsorption.

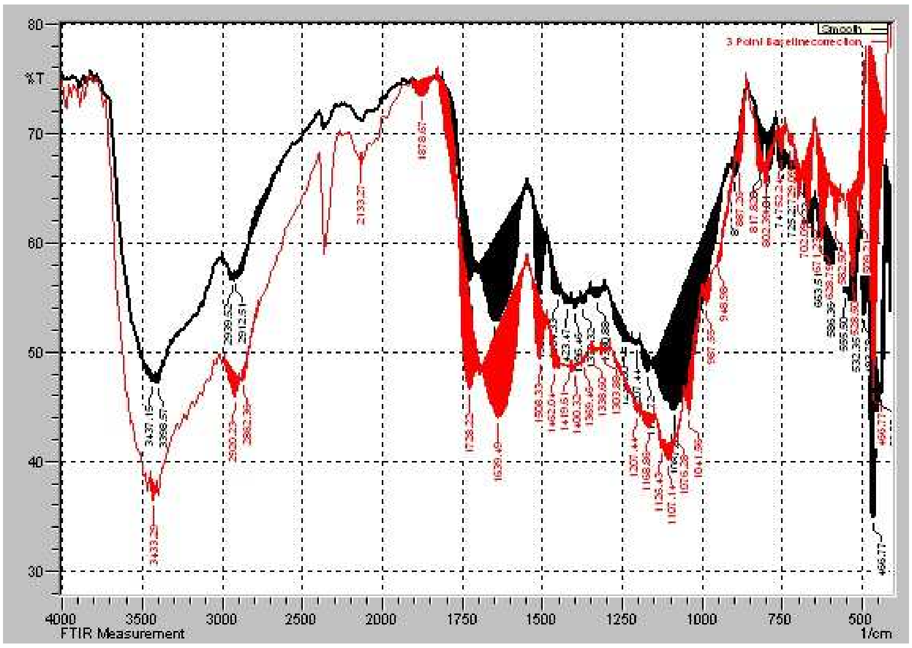

Figure13. FTIR spectra of RH (1) before, (2) after Pb^{+2} adsorption

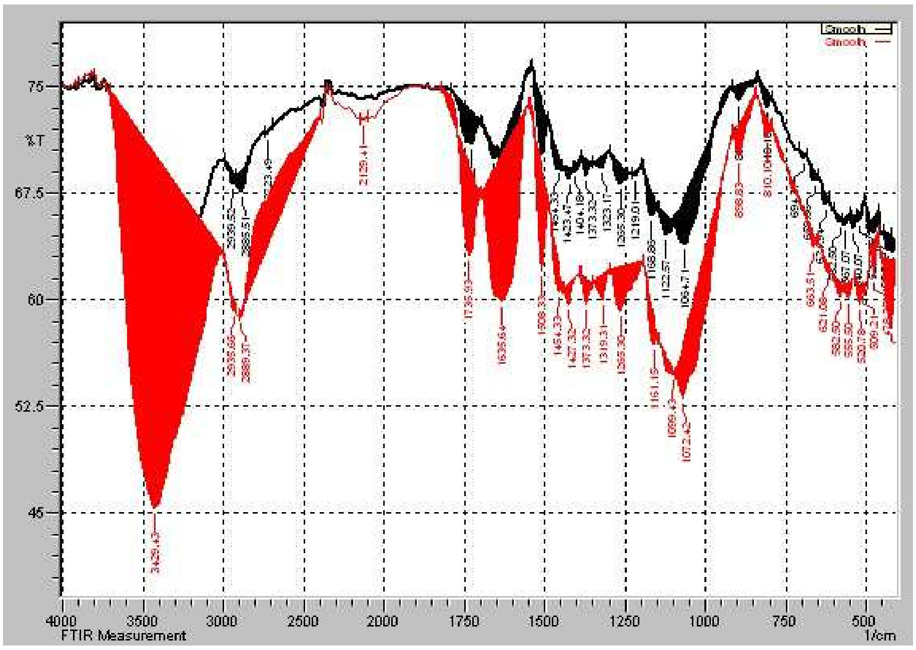

Figure14. FTIR spectra of SD (1) before, (2) after Pb^{+2} adsorption

4. Conclusions

In batch adsorption system, this study showed that locally available materials, such as RH and SD, can be used as efficient adsorbents as compared by commercial GAC for leadion removal. The pH experiments revealed that the governing factor affecting the adsorption characteristics of the selected adsorbents are competitively of the H+ ions with Pb^{2+} ions at very low pH values, maximum absorption at pH 5. Increase in mass of adsorbent lead to increase in Pb^{2+} adsorption due to increase in number of adsorption sites. The maximum uptake of Pb^{2+} obtained at an adsorbent dose of 2 g for all the adsorbents. Data demonstrated that PR had considerable potential for the removal of lead (II) from aqueous solution. Langmuir isotherm was fitted very well with experimental data. From the Langmuir isotherm, the maximum adsorption capacity for the lead(II) ions was found at 6.823, 263.044, and 10.046 mg/g onto GAC, RH, and SD, respectively. Optimum adsorption conditions for lead(II) ion removal are as follows: pH 5, contact time 270 min, and adsorbent dose 2 g.

The variation in sorption capacities between the various adsorbents could be linked to the character and concentration of surface group responsible for the adsorption of lead ions from solution. The kinetics of the Pb^{2+} adsorption on the different adsorbents was found to follow a first-orderrate mechanism. Thermodynamic calculations showed that the Pb^{2+} adsorption was spontaneous in nature. . The Gibbs free energy values were obtained as -8.408, -6.214, and -7.916 kJmol^{-1} which correspond, respectively, to GAC, RH, and SD. More studies are needed to investigate the applicability of these adsorbents under real condition such as industrial effluent treatment.

References

1. Paulino, A.T.; Tessari, J. A.; Nogami, E.M.; Lenzi, E.; Nozaki, J. (2005). *"Lipid-increase-induced-by-lead-accumulation-in-tilapia-Oreochromis-niloticus"*.Bulletin of Environmental Contamination and Toxicology, Vol. 75, No.1, pp. 42-49.
2. Johnson, P.M.. (1998). *"The genetic effects of environmental lead"*. Mutat. Res. Vol. 410, pp. 123-140.
3. WHO Guideline Values for Drinking Water Quality, Vol. 1, Recommendations, World Health Organization: Geneva; 1984; p. 81.
4. Horsfall, J.M.; Abia, A. A. (2003). *"Sorption of Cd (II) and Zn (II) ions from aqueous solutions by Cassava waste biomass (Manihot succulentcranes"*. Water. Res, Vol. 37, No. 20, pp. 4913-4923.
5. Reddad, Z.; Gerente, C.; Andeers, Y.; Pierrele, L.C. (2002). *"Adsorption of several metal ions onto a low cost biosorbent: kinetic and Equilibrium studies"*. Environ. SCI. Technol. Vol. 36, No. 9, pp. 2067-2073.
6. Paulino, A.T.; Simonato, J.I.; Garcia, J.C.; Nozaki, J. (2006). *"Characterization of Chitosan and chitin produced from silkworm chrysalis"*. Carbohydr.Polym. Vol. 64, pp. 98-103.
7. Tahir, S.S.; Rauf, N. J. (2003). *"Thermodynamic studies of Ni (II) sorption onto bentoite from aqueous solution"*. The Journal of Chemical Thermodynamics, Vol. 35 No. 12.
8. APHA, (1995). *"Standard methods for the examination of water & wastewater"*. 19th ed., American Public Health Association, Washington, DC.
9. Sulaymon A.H., Abbood D.W., Ali A.H., (2012). *"Removal of phenol and lead from synthetic wastewater by adsorption onto granular activated carbon in fixed bed adsorbers: Prediction of breakthrough curves"*. DWT J., Vol. 40, pp. 244–253.
10. Veglio F., Beolchini F., Prisciandano M., (2003). *"Sorption of copper by olive mill residues"*. Water Res., Vol. 37, pp. 4895–4903.
11. Vijayaraghavan K., and Yun YS., (2008). *"Biosorption of C.I. Reactive Black 5 from aqueous solution using acid-treated biomass of brown seaweed Laminaria sp"*. Dyes Pigm., Vol. 76, pp. 726–32.
12. Ho Y.S., (2004). *"Citation review of Lagergren kinetic rate equation on adsorption reactions"*. Scientometrics, Vol. 59, pp. 171–177.
13. H., Tang, W. Zhou, and L. Zhang., (2012).*"Adsorption isotherms and kinetics studies of malachite green on chitin hydrogels"*. J. Hazard. Mater, pp. 218– 225.
14. Quintelas, C., Fernandes, B., Castro, J., Figueiredo, H., Tavares, T.,(2008). *"Biosorption of Cr(VI) by three different bacterial species supported on granular activated carbon—A comparative study"*. J, Hazardous Materials, Vol. 153, pp. 799–809.
15. Aldre, J., Morais, B., Shiva, P., Valderi D. L., Antonio, G. S., (2007). *"Biosorption of heavy metals in upflow sludge columns"*. Bioresource Technology, Vol. 98 , pp. 1418–1425.

16. M.A. Martin-Lara, Herninz F., Calero M., Blzquez G., and Tenorio G., (2009). *"Surface chemistry evaluation of some solid wastes from olive-oil industry used for lead removal from aqueous solutions"*. Biochem. Eng. J., Vol. 44, pp. 151-159.
17. Heidari, A., Younesi, H., Mehraban, Z., (2009). *"Removal of Ni (II), Cd(II), and Pb(II) from a ternary aqueous solution by amino functionalized mesoporous and nano mesoporous silica"*. Chem. Eng. J., Vol. 153, pp. 70–79.
18. Kumar, P.S. And Kirthika, K., (2010). *"Kinetics and equilibrium studies of* Zn^{+2} *ion removal from aqueous solutions by use of natural wast"*. Electronic Journal of Environmental, Agricultural and Food Chemistry, Vol. 9, No. 1, pp. 262-274.
19. Dorris K.L., B. Yu, Zhang Y., Shukla A., Shukla S.S., (2000). *"The removal of heavy metal from aqueous solutions by sawdust adsorption-removal of copper"*. J. Hazard. Mater., Vol. B80, pp. 33–42.
20. Tlaiaa, Y.S., (2014). *"Using of Coagulation and Adsorption Treatment Processes as a Single and in Combination for Removal of Reactive Textile Dyes from Simulated Wastewater"*.MSc. Thesis, University of AL-Mustansiriayah, College of Engineering.
21. Chantawong V., Harvey N.W. and Bashkin V.N., (2001). *"Comparison of heavy metal adsorptions by thai kaolin and ballclay"*. Asian Journal of Energy & Environmental.Vol. 1, pp. 33–48.
22. Y. Swesi, A. Elmeshergi, A. Elalem and W. Alfoghy, (2013). *"Utilization of Cement Kiln Dust in AdsorptionTechnology", International Journal of Chemical*, Materials Science and Engineering. Vol. 7, pp. 14-16.
23. M. A. Awan, I. A. Qazi, I. Khal., (2003). *"Removal of heavy metals through adsorption using Sand"*. Journal of environmental science, Vol. 15, pp. 413-416.
24. Hamadi N. J. , Mohammed A. A., A. Ali H.,(2014). *"Removal of* Pb^{2+}, Cu^{2+} *and* Cd^{2+} *Metals from Simulated Wastewater in Single and Competitive System Using Locally Porcelanite"*. International Journal of Engineering Sciences & research, Vol. 3, No.7, pp. 2277- 9655
25. Bassim Hameed Graimed Ziad T. Abd Ali, (2013). *"Thermodynamic and Kinetic Study of the Adsorption of Pb (II) from Aqueous Solution Using Bentonite and Activated Carbon"*. Al-Khwarizmi Engineering Journal, Vol. 9, No. 2, pp. 48 - 56.
26. Wang Xuejiang , Chen Ling , Xia Siqing , Zhao Jianfu , Jean-Marc Chovelon , Nicole Jaffrezic Renault,(2006). *"Biosorption of Cu(II) and Pb(II) from aqueous solutions by dried activated sludge"*. Minerals Engineering, Vol.19, pp. 968–971.
27. Sirvastava SK., Tyagi R., Pant N., (1989). *"Adsorption of heavy metals on carbonaceous material developed from the waste slurry generated in local fertilizer plants"*. Water Res. Vol. 45, pp. 654–664.
28. Sulaymon A.H., Abbood D.W., Ali A.H., (2011). *"Competitive adsorption of phenoland lead from synthetic wastewater onto granular activated carbon"*. J. Environ. Sci. Eng. Vol. 5, pp.1389–1399.

29. Safa, Y. and Bhatti, H.N., (2011). *Adsorptive Removal of Direct Dyes by Low Cost Rice Husk,* African Journal of biotechnology, Vol. 10, No. 16, pp. 3128-3142.
30. Ansari,R., and Mosayebzadeh, Z.,(2010). *"Removal of basic dye methylene blue from aqueous solutions using sawdust and sawdust coated with polypyrrole"*. J. Iran Chem. Soc., Vol. 7, pp. 339-350.